Two Polyoxometalate-based Host-guest Compounds: Synthesis, Crystal Structure and Catalytic Performance①

WANG Song-Xia[a, b] WANG Sa-Sa[b] WU Xiao-Yuan[b]
YANG Wen-Bin[b] LU Can-Zhong[b, c②]

[a] (*Fujian Normal University, Fuzhou* 350007, *China*)

[b] (*CAS Key Laboratory of Design and Assembly of Functional Nanostructures, and Fujian Provincial Key Laboratory of Nanomaterials, Fujian Institute of Research on the Structure of Matter, Chinese Academy of Sciences, Fuzhou* 350002, *China*)

[c] (*University of Chinese Academy of Sciences, Beijing* 100049, *China*)

ABSTRACT Two polyoxometalate-based host-guest compounds, $(HL_1)_2(HPW_{12}O_{40})\sim11H_2O$ (**1**), $(HL_2)_3(PW_{12}O_{40})\ 3H_2O$ (**2**) (L_1 = guanine, L_2 = 2-(1H-1,2,4-triazol-3-yl)pyridine), were synthesized under hydrothermal conditions and characterized by EA, PXRD, TG, FT-IR and X-ray single-crystal diffraction. Compound **1** crystallizes in trigonal space group *P*-3 with a = 18.2917(5), b = 18.2917(5), c = 13.5441(5) Å, V = 3924.5(3) Å^3, Z = 3, M_r = 3383.26 g/mol, ρ_{calc} = 4.036 g/cm^3, F(000) = 4137, μ = 48.532 mm^{-1}, *GOOF* = 1.062, the final R = 0.0713 and wR = 0.1865 for 9037 observed reflections with $I > 2\sigma$(I). Compound **2** crystallizes in trigonal space group *R*-3 with a = 19.0017(6), b = 19.0017(6), c = 25.6361(9) Å, V = 8016.2(6) Å^3, Z = 6, M_r = 3372.45 g/mol, ρ_{calc} = 4.188 g/cm, F(000) = 8886, μ = 47.644 mm^{-1}, *GOOF* = 1.077, the final R = 0.0380 and wR = 0.0976 for 5904 observed reflections with $I > 2\sigma(I)$. These two compounds can catalyze selective oxidation of aniline with H_2O_2 as the oxidant. Under optimal conditions, the conversion of aniline with compound **1** can reach up to 91.25%, and the selectivity of nitrosobenzene is 78.81%.

Keywords: polyoxometalates, catalytic oxidation, aniline, nitrosobenzene;
DOI: 10.14102/j.cnki.0254-5861.2011-3226

1 INTRODUCTION

Polyoxometalate (POM) is a kind of metal-oxygen clusters traditionally consisting of transition elements of Mo, W, V, Nb and Ta. They have been widely used in many fields including catalysis due to their unique properties[1-3]. Their catalytic performance can be adjusted by changing the molecular composition and structure[4-6], and therefore they can meet the requirements of specific catalytic processes. So far, there are several industrial processes with POMs or related heteropolyacids (HPAs) as homogeneous catalysts[7]. However, the excellent solubility of the used POMs/HPAs in these processes suggests that the recovery and reuse of catalysts are challenging issues[8]. In order to address these issues, researchers have put great effort on immobilizing them on various supports and solidifying them by cation exchange or covalent modification of the anion[9-12]. The resulting heterogeneous catalysts are usually bulk phase catalysts, implying the disadvantage of the low dispersity of catalytically active sites[13]. Moreover, the loss of activity of POM anion often happens in the catalytic process owing to the aggregation and/or degradation of POM anion. POM-based host-guest compounds usually have high stability and unique catalytic properties profiting from the weak interaction between host and guest, such as anion-π interaction, hydrogen bond, *etc.* The introduction of organic moiety as the host causes the solidification of POM catalyst. Furthermore, the POM units in such compounds are distributed uniformly, suggesting that high catalytic activity is probably achieved[14-16].

Received 19 April 2021; accepted 11 June 2021 (**CCDC 2073305 for 1 and 2073431 for 2**)

① This work was supported by the Key Research Program of Frontier Science, CAS (QYZDJ-SSW-SLH033), the Strategic Priority Research Program of the Chinese Academy of Sciences (XDB20000000) and the National Natural Science Foundation of China (21773247, 21521061, 21875252, 52073286)

② Corresponding author. E-mail: czlu@fjirsm.ac.cn

In the past few decades, the oxidation of harmful organic substrates into corresponding oxygen-containing derivatives using hydrogen peroxide as the oxidant has attracted great attention[17]. Aniline is regarded as a carcinogen. The selective oxidation of aniline not only eliminates the pollutant, but also realizes the recycle of waste[18]. Nitrosobenzene, one of the products of the reaction, is a valuable fine chemical that has been used for polymer, drug, dye and fragrance production[19, 20].

In this work, two POM-based host-guest compounds, $(HL_1)_2(HPW_{12}O_{40})\sim 11H_2O$ (**1**) and $(HL_2)_3(PW_{12}O_{40})\ 3H_2O$ (**2**), were successfully synthesized and used as heterogeneous catalysts for the selective oxidation of aniline to nitrosobenzene with H_2O_2 as the oxidant. Under optimized conditions, compound **1** gave a conversion of aniline of 91.25%, and a selectivity of nitrosobenzene of 78.81%. Compound **2** gave a conversion of aniline of 88.18% and a selectivity of nitrosobenzene of 69.09%.

2 EXPERIMENTAL

2. 1 Materials and methods

All reagents and solvents were of AR grade and used without further purification. Elemental analysis for C, H and N was carried out on an Elementar Vario EL CUBE elemental analyzer. Powder X-ray diffraction (PXRD) measurements were carried out at room temperature using a Rigaku MiniFlex600 powder diffractometer with Cu$K\alpha$ radiation (λ = 1.5405 Å) with a scan speed of 0.2 s per step and a step size of 0.02 (2θ). Thermogravimetric analysis (TGA) was performed by Mettler-Toledo TGA/DSC 1 STARe. The Fourier Transform infrared spectroscopy (FT-IR) spectra (4000～400 cm^{-1}) were recorded by using KBr pellet on a Bruker VERTEX70 FTIR spectrometer. The catalysis data were collected on by gas chromatography (Agilent 6820).

2. 2 Syntheses of compounds 1 and 2

Synthesis of compound 1 The solution containing 0.6 mmol $H_3PW_{12}O_{40}\cdot nH_2O$, 0.3 mmol guanine and 8 mL H_2O was stirred continuously for half an hour at ambient temperature, and then smoothly transferred to an autoclave lined with Teflon and kept at 120 ℃ for 72 h. After cooling down to room temperature, massive orange crystals were obtained (yield: 0.32 g, 31.55% based on guanine). EA calculated (%): C, 3.55; H, 1.03; N, 4.14. Found (%): C, 4.09; H, 0.75; N, 4.86.

Synthesis of compound 2 compounds **2** was synthesized with the same method as that for compound **1**, except replacing guanine with 2-(1H-1,2,4-triazol-3-yl)pyridine. Massive colorless crystals were obtained (yield: 0.32 g, 31.66% based on 2-(1H-1,2,4-triazol-3-yl)pyridine). EA calculated (%): C, 7.48; H, 0.80; N, 4.98. Found (%): C, 7.63; H, 0.83; N, 5.13.

2. 3 Crystallographic structure determination

Crystallography data were obtained from Rigaku Super Nova with CCD detector and X-ray source of Cu$K\alpha$ radiation (λ = 1.54184 Å). The structure was solved by direct methods with SHELXL Crystallographic Software. All H atoms were refined isotropically as a riding mode by using the default SHELXTL parameters. In the refinements, there are large solvent accessible voids in the crystal structure of compound **1**, indicating that more water molecules should exist in the structure which cannot be found from the weak residual electron peaks, and this structure was treated by using the SQUEEZE method in PLATON.

Crystal data for **1** ($C_{10}H_{13}N_{10}O_{42}PW_{12}\sim 11H_2O$): space group P-3, M_r = 3383.26 g/mol, a = 18.2917(5) b = 18.2917(5), c = 13.5441(5) Å, V = 3924.5(3) $Å^3$, Z = 3, T = 293(2) K, μ(Cu$K\alpha$) = 48.532 mm^{-1}, ρ_{calc} = 4.036 g/cm^3, 9037 reflections measured ($6.53\leqslant 2\theta\leqslant 146.52°$), 5097 unique ($R_{int}$ = 0.0629, R_{sigma} = 0.0670), final R = 0.0713 ($I \geqslant 2\sigma(I)$) and wR = 0.1960 (all data).

Crystal data for **2** ($C_{21}H_{27}N_{12}O_{43}PW_{12}$): space group R-3, M_r = 3372.45 g/mol, a = 19.0017(6), b = 19.0017(6), c = 25.6361(9) Å, V = 8016.2(6) $Å^3$, Z = 6, T = 293(2) K, μ(Cu$K\alpha$) = 47.644 mm^{-1}, ρ_{calc} = 4.188 g/cm^3, 5904 reflections measured ($6.38\leqslant 2\theta\leqslant 149.79°$), 3507 unique ($R_{int}$ = 0.0265, R_{sigma} = 0.0299), the final R = 0.0380 ($I \geqslant 2\sigma(I)$) and wR = 0.1004 (all data).

2. 4 Catalytic oxidation experiment

The general procedure of catalytic oxidation of aniline to nitrosobenzene is as follows: 0.017 mmol catalysts (**1** and **2**), 0.5 mmol aniline, 0.75 mmol H_2O_2, and 2 mL acetonitrile were added into the reaction tube in succession. Then, the tube was heated to 60 ℃ and kept for 1.5 h. After cooling down to room temperature, the organic phase of the reaction mixture was extracted by diethyl ether, dried by anhydrous Na_2SO_4, and analyzed by gas chromatography. The dosage of controlling catalysts was equal to that in the title compounds.

3 RESULTS AND DISCUSSION

3. 1 X-ray crystal structure

High-quality crystals of compounds **1** and **2** were obtained by hydrothermal method, and analyzed by X-ray single-crystal diffraction. Compounds **1** and **2** are host-guest structures viewed from their packing model (Fig. 1c, 1f). Compound **1** crystallizes into the trigonal space group *P*-3. The POM anion and guanine are interacted by weak intermolecular forces including hydrogen bond and anion-π (Fig. 1a). The POM anions can be divided into two types: A and B. POM A interacts with guanine through two types of hydrogen bonds (C_2–$H_2\cdots O_5$, 3.400(3) Å; N_{11}–$H_{11B}\cdots O_{11}$, 2.930(3) Å) and anion-π (the distance between the oxygen atom on POM A and the guanine is 3.473 Å) (Fig. 1a, Table 1). POM B and 6 surrounding guanine molecules are connected to each other through anion-π interaction (the distance between the oxygen atom on POM B and guanine is 3.262 Å) (Fig. 1b). The packing model exhibits that compound **1** can be viewed as a host-guest compound (Fig. 1c). Compound **2** crystallizes into the trigonal space group *R*-3. The POM anion and 2-(1H-1,2,4-triazol-3-yl)pyridine are also interacted with each other by three types of hydrogen bonds (C_1–$H_1\cdots O_1$, 3.391 Å; C_5–$H_5\cdots O_{14}$, 3.461 Å; N_2–$H_2\cdots O_6$, 2.970 (11) Å) and anion-π (the distance between the oxygen atom on POM and 2-(1H-1,2,4-triazol-3-yl)pyridine is in the range of 3.338~3.724 Å) (Fig. 1d, Table 2). In the structure, each POM is surrounded by 12 2-(1H-1,2,4-triazol-3-yl)pyridine molecules (Fig. 1e). The packing model exhibits that compound **2** is also a host-guest compound (Fig. 1f). It is deduced that the weak interactions between POMs and organic moieties in compounds **1** and **2** may have an impact on their catalytic performance.

Table 1. Hydrogen Bonds for Compound 1 (Å and °)

D–H···A	D–H	H···A	D···A	D–H···A
C(2)–H(2)···O(5)[1]	0.93	2.50	3.400(3)	164
N(11)–H(11B)···O(11)	0.87	2.30	2.930(3)	129

Symmetry code: [1] *–y, x – y, z*

Table 2. Hydrogen Bonds for Compound 2 (Å and °)

D–H···A	D–H	H···A	D···A	D–H···A
N(2)–H(2)···O(6)[1]	0.86	2.13	2.970(11)	165
C(1)–H(1)···O(1)[2]	0.93	2.50	3.391	161
C(5)–H(5)···O(14)[3]	0.93	2.61	3.461	153

Symmetry codes: [1]*x–y*+1, *x*, *–z*+1; [2]*x–y*+1, *x*, *–z*+1; [3]*y*, *–x*+*y*+1, *–z*+1

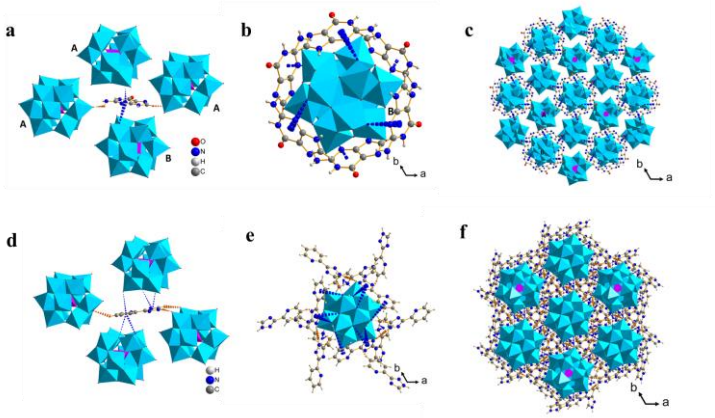

Fig. 1. a: L_1 interacted POMs in 1 (The orange dashed line is hydrogen bonding, and the blue dashed line is anion-π interaction); b: POM B surrounded by L_1 in 1; c packing model of 1; d: L_2 interacted POMs in 2; e: POM guest surrounded by L_2 in 2; f: packing model of 2. (In order to make the image clear, and the crystal water molecules are deleted)

3. 2 Infrared spectrum

The FT-IR spectrum of compound **1** in the range of 400~4000 cm^{-1} was carried out (Fig. 2a). The four characteristic vibration bands of the Keggin skeleton are in the low wavenumber region, respectively at 1080 cm^{-1} (ν(P–O)), 987 cm^{-1} (ν(W–Ot)), 898 cm^{-1} (ν(W–Ob)) and 798 cm^{-1} (ν(W–Oc))[21]. In addition, the absorption peaks at 3354 and 3145 cm^{-1} are attributed to $\nu(N–H_{(NH2)})$ and $\nu(N–H_{(NH)})$; the absorption peak at 1693 cm^{-1} is attributed to ν(amide C=O); the absorption peak at 1558 cm^{-1} is due to ν(ring

double bonds); the absorption peaks at 1475 and 1413 cm^{-1} are assigned to *v*(ring vibration); the absorption peaks at 827 and 783 cm^{-1} result from to the skeletal vibration of L1; the absorption peak at 609 cm^{-1} is attributed to -CH deformations, all of which can confirm the presence of guanine in **1**[22]. In short, the results of IR spectroscopy are consistent with the single crystal structure analysis.

The FT-IR spectrum of compound **2** in the range of 400~4000 cm^{-1} was also carried out (Fig. 2b). The characteristic vibration bands of the Keggin framework of compound **2** are in the low wavenumber region at 1080 cm^{-1} (*v*(P–O)), 993 cm^{-1} (*v*(W–Ot)), 893 cm^{-1} (*v*(W–Ob)) and 808 cm^{-1} (*v*(W–Oc)) correspondingly. In addition, the absorption peaks at 3481 and 3263 cm^{-1} are attributed to *v*(N–H); that at 3113 cm^{-1} results from *v*(C–H); those at 1637 and 1460 cm^{-1} are due to *v*(C=C) and *v*(C=N); and those at 1342 and 1299 cm^{-1} are assigned to *v*(C=N), all of which can confirm the presence of 2-(1H-1,2,4-triazol-3-yl)pyridine) in **2**. In short, the results of IR spectroscopy are consistent with the single crystal structure analysis.

3. 3 Powder X-ray diffraction

The phase purity of compounds **1** and **2** is determined by good agreement between the experimental X-ray diffraction patterns of **1** and **2** and the simulated single-crystal X-ray diffraction data, but the intensity is different, which is mainly due to the variation of the preferred orientation of the powder sample for the powder diffraction data (Fig. 2c, 2d)[23].

3. 4 Thermogravimetric analysis

The TGA of compound **1** exhibits two-step weight loss. The first one from 32 to 200 ℃ is 3.88%, which is attributed to the removal of lattice water molecules. When heated to 400 ℃, continuous weight loss appears, indicating that the organic ligands and POM units begin to decompose (Fig. 2e).

Compound **2** also shows two-step weight loss. The weight loss for the first step from 32 to 209 ℃ is 1.71%, which is equivalent to the departure of 3 lattice water molecules. When heated to 400 ℃, continuous weight loss occurs, suggesting that the organic ligands and POM units start to decompose (Fig. 2f).

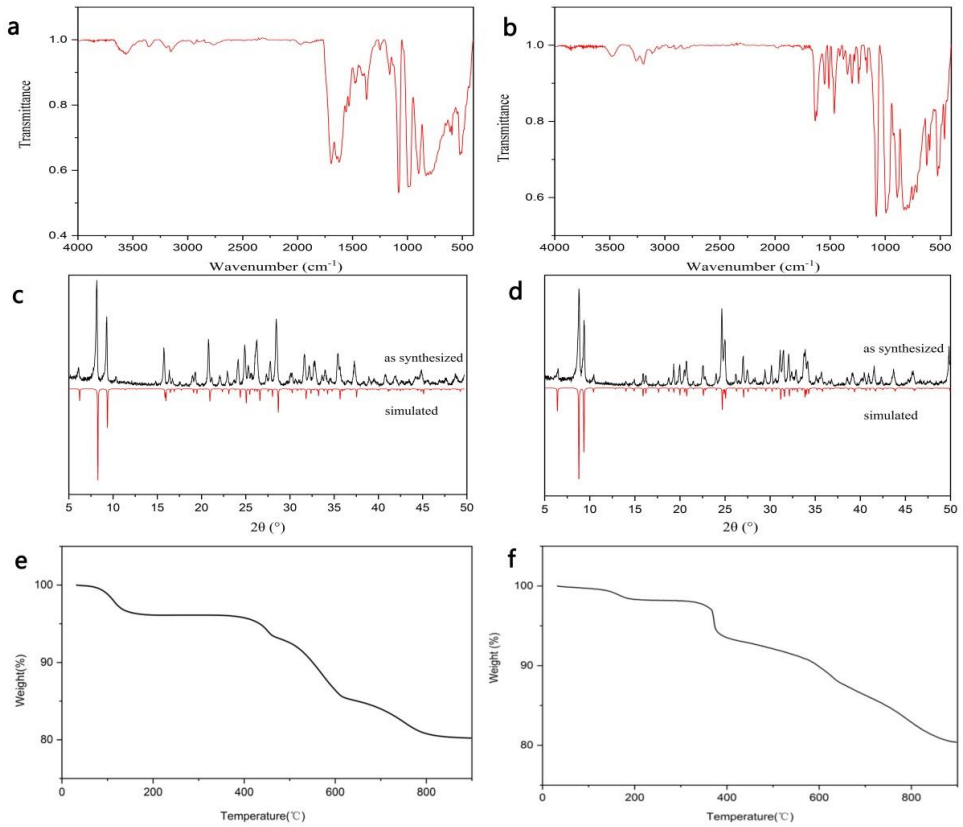

Fig. 2. a: FT-IR spectra of 1; b: FT-IR spectra of 2; c: PXRD patterns of 1; d: PXRD patterns of 2; e: TG curve of compound 1; f: TG curve of compound 2

3. 5 Oxidation catalysis

In order to evaluate the catalytic performance of compounds **1** and **2**, we have performed the selective oxidation of aniline with different catalysts in acetonitrile solvent with H_2O_2 as the oxidant (Fig. 3). In the absence of catalysts, the conversion of aniline is as low as 42.43%, and only a trace of nitrosobenzene is observed. However, in the presence of catalyst **1** (**2**), the conversion of aniline is 91.25% (88.31%) and the selectivity towards nitrosobenzene reaches up to 78.81% (63.33%). The results suggest that compounds **1** and **2** can effectively promote the reaction. Additionally, the catalysts can be partially recovered after reaction. One of the starting materials for **1** and **2**, $H_3PW_{12}O_{40}$, shows a conversion of 96.89% and a selectivity towards nitrosobenzene of 63.45%. Although the results are comparable with those of compounds **1** and **2**, the recovery of the homogeneous catalyst cannot be realized. Other starting materials for **1** and **2**, guanine and 2-(1H-1,2,4-triazol-3-yl)pyridine, show negligible catalytic performance compared with the results for the reaction without catalyst. The related heterogeneous catalyst WO_3 gives aniline conversion of 85.82% and selectivity towards nitrosobenzene of 41.14% under identical conditions, indicative of the advantages of compounds **1** and **2**.

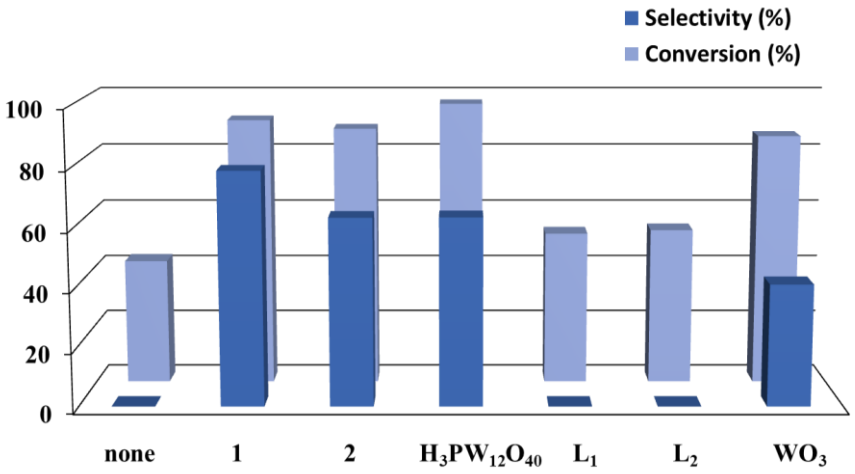

Fig. 3. The oxidation of aniline with different catalysts (Condition: aniline 0.5 mmol, acetonitrile 2 mL, H_2O_2 0.75 mmol, 60 °C, 1.5 h. selectivity: selectivity to nitrosobenzene)

3. 6 Catalyst mechanism

The possible reaction mechanism is proposed. Initially, oxidative POMs react with aniline to realize the oxidation of aniline, accompanied by the reduction of POMs. Then, the reduced POM catalysts are reoxidized by H_2O_2 to regenerate oxidative POMs (Fig. 4)[19].

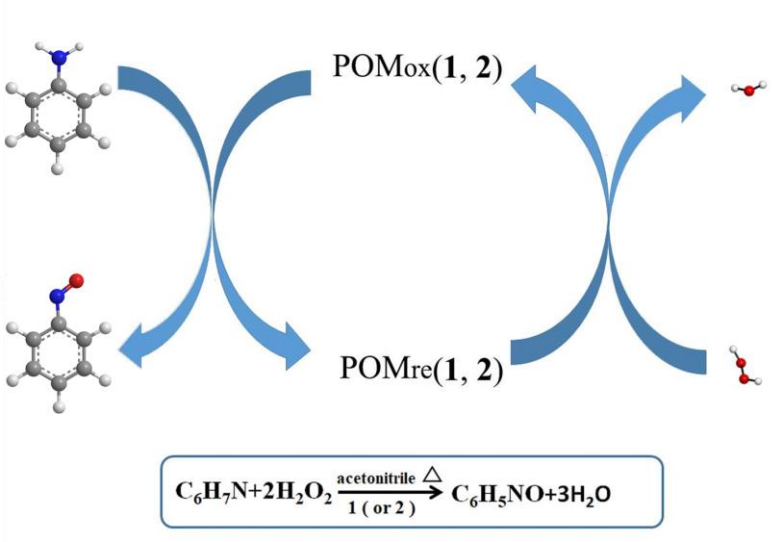

Fig. 4. Proposed mechanism for the selective oxidation of aniline

4 CONCLUSION

In summary, we have synthesized two new host-guest compounds **1** and **2**, and evaluated their catalytic properties using the selective oxidation of aniline as the probe reaction. The results indicate that they can efficiently promote the selectively oxidation of aniline towards nitrosobenzene. The work provides a useful reference for the synthesis of catalytic materials composed of nitrogen heterocyclic organic compounds and polyoxometalates.

REFERENCES

(1) Li, T. F.; Miras, H. N.; Song, Y. F. Polyoxometalate (POM)-layered double hydroxides (LDH) composite materials: design and catalytic applications. *Catalysts* **2017**, 7, 260.

(2) Pope, M. T.; Müller, A. *Polyoxometalate Chemistry: from Topology via Self-assembly to Applications* **2001**.

(3) Mizuno, N.; Yamaguchi, K.; Kamata, K. Epoxidation of olefins with hydrogen peroxide catalyzed by polyoxometalates. *Coordin. Chem. Rev.* **2004**, 249, 1944–1956.

(4) Miras, H. N.; Yan, J.; Long, D. L.; Cronin, L. Engineering polyoxometalates with emergent properties. *Chem. Soc. Rev.* **2012**, 41, 7403–7430.

(5) Barteau, M. A.; Lyons, J. E.; Song, I. K. Surface chemistry and catalysis on well-defined oxide surfaces: nanoscale design bases for single-site heterogeneous catalysts. *J. Catal.* **2003**, 216, 236–245.

(6) Deshlahra, P.; Carr, R. T.; Chai, S. H.; Iglesia, E. Mechanistic details and reactivity descriptors in oxidation and acid catalysis of methanol. *ACS Catal.* **2015**, 5, 666–682.

(7) Wang, S. S.; Yang, G. Y. Recent advances in polyoxometalate-catalyzed reactions. *Chem. Rev.* **2015**, 115, 4893–4962.

(8) Kumar, A.; Gupta, A. K.; Devi, M.; Gonsalves, K. E.; Pradeep, C. P. Engineering multifunctionality in hybrid polyoxometalates: aromatic sulfonium octamolybdates as excellent photochromic materials and self-separating catalysts for epoxidation. *Inorg. Chem.* **2017**, 56, 10325–10336.

(9) Wilke, T.; Barteau, M. A. Dehydration and oxidation of alcohols by supported polyoxometalates: effects of mono- and multivalent cation exchange on catalyst acidity and activity. *Ind. Eng. Chem. Res.* **2019**, 58, 14752–14760.

(10) Wilke, T.; Barteau, M. A. Cation exchange effects on methanol oxidation and dehydration by supported polyoxometalates. *J. Catal.* **2019**, 371, 357–367.

(11) Uchida, S. Frontiers and progress in cation-uptake and exchange chemistry of polyoxometalate-based compounds. *Chem. Sci.* **2019**, 10, 7670–7679.

(12) Derouich, S. G.; Rinfray, C.; Izzet, G.; Pinson, J.; Gallet, J. J.; Kanoufi, F.; Proust, A.; Combellas, C. Control of the grafting of hybrid polyoxometalates on metal and carbon surfaces: toward submonolayers. *Langmuir.* **2014**, 30, 2287–2296.

(13) Zhang, M.; Li, H. J.; Zhang, J. H.; Lv, H. J.; Yang, G. Y. Research advances of light-driven hydrogen evolution using polyoxometalate-based catalysts. *Chin. J. Catal.* **2021**, 42, 855–871.

(14) Gong, Y.; Hu, C. W.; Liang, H. Research progress in synthesis and catalysis of polyoxometalates. *Prog. Nat. Sci-Mater.* **2005**, 15, 385–394.

(15) Liu, P.; Wang, C. H.; Li, C. Epoxidation of allylic alcohols on self-assembled polyoxometalates hosted in layered double hydroxides with aqueous H_2O_2 as oxidant. *J. Catal*. **2009**, 262, 159–168.

(16) Li, J.; Huang, Y.; Han, Q. X. Decatungstate incorporated metal-organic framework for degradation of Rhodamine B under sunlight irradiation. *Chin. J. Struct. Chem.* **2013**, 32, 1897–1903.

(17) Sakaue, S.; Sakata, Y.; Nishiyama, Y.; Ishii, Y. Oxidation of aliphatic and aromatic amines with hydrogen peroxide catalyzed by peroxoheteropoly oxometalates. *Chem. Lett*. **1992**, 21, 289–292.

(18) Tang, G. Q.; Sun, J.; Wu, F. K.; Sun, Y.; Zhu, X. W.; Geng, Y. J.; Wang, Y. S. Organic composition of gasoline and its potential effects on air pollution in North China. *Sci. China Chem.* **2015**, 58, 1416-1425.

(19) Trautwein, G.; El Bakkali, B.; Alcaniz-Monge, J.; Artetxe, B.; Reinoso, S.; Gutierrez-Zorrilla, J. M. Dimeric assemblies of lanthanide-stabilised dilacunary Keggin tungstogermanates: a new class of catalysts for the selective oxidation of aniline. *J. Catal*. **2015**, 331, 110–117.

(20) Gowenlock, B. G.; Richter-Addo, G. B. Preparations of C-nitroso compounds. *Chem. Rev.* **2004**, 104, 3315–3340.

(21) Rao, G. R.; Rajkumar, T. Investigation of 12-tungstophosphoric acid supported on $Ce_{0.5}Zr_{0.5}O_2$ solid solution. *Catal. Lett.* **2008**, 120, 261–273.

(22) Oza, M. D.; Meena, R.; Prasad, K.; Paul, P.; Siddhanta, A. K. Functional modification of agarose: a facile synthesis of a fluorescent agarose-guanine derivative. *Carbohyd. Polym.* **2010**, 81, 878–884.

(23) Ma, W. D.; Li, H. L.; Yang, G. Y. A new 3-D supramolecular framework built by Co_4-substituted sandwiched phosphortungstates, organoamines and Co-complexes: synthesis, structure, and property. *Chin. J. Struct. Chem.* **2019**, 38, 1585–1592.